Journal of Instrumentation

Fine structure of angular distribution of x-ray transition radiation from multilayered radiator in Geant4

Published by IOP Publishing for Sissa Medialab

Received: *January 15, 2020*
Accepted: *April 14, 2020*
Published: *June 8, 2020*

XIII International Symposium on Radiation from Relativistic Electrons in Periodic Structures — RREPS-19
September 16–20, 2019
Belgorod, Russian Federation

Fine structure of angular distribution of x-ray transition radiation from multilayered radiator in Geant4

A.A. Savchenko,[a,b,c,1] **A.A. Tishchenko,**[a,b,c] **D.Yu. Sergeeva,**[a,b,c] **N. Belyaev,**[a] **M. Cherry,**[f] **F. Dachs,**[d,e] **S. Doronin,**[a] **K. Filippov,**[a] **P. Fusco,**[g,h] **F. Gargano,**[h] **S. Konovalov,**[i] **F. Loparco,**[g,h] **V. Mascagna,**[j,k] **M.N. Mazziotta,**[h] **S. Nechaeva,**[a] **D. Ponomarenko,**[a] **A. Romaniouk,**[a] **E.J. Schioppa,**[d] **S. Smirnov,**[a] **Y. Smirnov,**[a] **M. Soldani,**[j,k] **P. Spinelli,**[g,h] **M.N. Strikhanov,**[a] **P. Teterin,**[a] **V.O. Tikhomirov,**[i] **K. Vorobev**[a] **and K. Zhukov**[i]

[a] *National Research Nuclear University "MEPhI", Moscow, Russia*
[b] *National Research Center "Kurchatov Institute", Moscow, Russia*
[c] *Belgorod National Research University, Belgorod, Russia*
[d] *CERN, Geneve, Switzerland*
[e] *Technical University of Vienna, Vienna, Austria*
[f] *Lousiana State University, Bâton-Rouge, U.S.A.*
[g] *University of Bari, Bari, Italy*
[h] *INFN — Sezione di Bari, Bari, Italy*
[i] *Lebedev Physical Institute, Moscow, Russia*
[j] *INFN — Sezione di Milano Bicocca, Milan, Italy*
[k] *University of Insubria, Como, Italy*

E-mail: aasavchenko1@mephi.ru

Abstract: The present version of the Transition Radiation (TR) simulation module implemented in the Geant4 toolkit describes very well experimental data for the TR energy distribution; however, it does not allow reproducing the details of angular distribution at small angles. In order to solve this problem, corrections to the existing x-ray TR module in Geant4 are proposed. With these corrections, the results of the simulations are in a good agreement with the angular TR distributions predicted by theory and obtained in the test beam measurements using a 480 um Si pixel detector and Mylar radiator.

Keywords: Cherenkov and transition radiation; Detector modelling and simulations I (interaction of radiation with matter, interaction of photons with matter, interaction of hadrons with matter, etc); Transition radiation detectors; Interaction of radiation with matter

[1] Corresponding author.

https://doi.org/10.1088/1748-0221/15/06/C06024

Contents

2020 JINST 15 C06024

1 Introduction

Nowadays in high energy physics it is conventional to use powerful toolkit for computer simulations. One of the most advanced and popular simulation tools is Geant. It has been developed by the Geant Collaboration at CERN and other scientific centres since 1974. The C++ version of Geant is Geant4 [1–3], which has become the leading toolkit for computer simulations in nuclear and radiation physics: accelerator physics [4, 5], high energy physics [6–12], medical physics [13, 14], space studies [15, 16], etc.

The current version of Geant4 (Geant 10.6.p01) includes an x-ray transition radiation (TR) module, which is based on the theory developed by Garibian [17]. Transition radiation emitted when a charged particle crosses the boundary between two different media was predicted theoretically by Ginzburg and Frank in 1945 [18]. TR is widely used in particle detectors [19–24] at accelerators in so-called transition radiation trackers/detectors [25–27]: e.g., TRT in ATLAS, TRD in ALICE (LHC, CERN), CBM (FAIR), etc.

The x-ray TR module in Geant4 uses Monte-Carlo algorithm implemented in the toolkit by Grichine and others [28–31]. In a recent paper [32] we confirmed that the agreement between theory and simulations in Geant4 is perfect in what concerns the spectral distribution of x-ray TR. Along with that we have shown that the angular distributions diverge for small angles, at which Geant4 cannot reproduce the fine structure of the angular distribution, namely, the sharp peaks at small angles. As these peaks were observed experimentally [33–37], and their positions coincide perfectly with the analytical calculations [32], we infer that the x-ray TR module in Geant4 needs refining. In fact, running ahead we can say the tool is so powerful and flexible that only minimal corrections are needed to improve it.

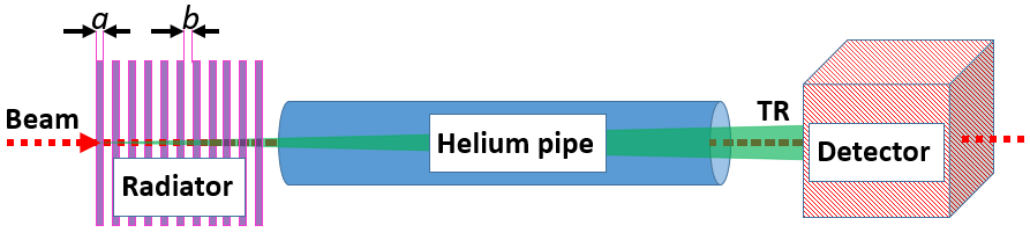

Figure 1. Scheme of TR detector for both angular and spectral measurements. Primary particle beam passes through the TR radiator, which is a periodical structure consisting of foils with the width a (magenta) and gas gaps of the width b between them, then along with generated TR photons (green areas) through the helium pipe and hits the detection system — a semiconducting pixel or strip detector.

2 Geant4 simulations of TR detector

The x-ray TR module included in Geant4 allows simulating x-ray photons generated by charged particles passing through a radiator. There are several radiator models implemented in the module. The most general model describes irregular radiator consisting of the films and gas gaps with fluctuating thicknesses. Most frequently used model, however, is a regular radiator — the radiator with regularly spaced gaps between films. Simulations for the regular one are 10 times faster in comparison with the irregular radiator even for almost zero irregularity. This is because the numerical code for an irregular radiator contains additional numerical integration. Besides, as we showed in [32], the model of regular radiator does describe well TR spectra, both experimental and theoretical. So, below we consider the regularly spaced radiator model.

The experimental setup tested in the SPS H8 beam line at CERN with different particles and radiators [34–37] is shown in figure 1. Primary particles cross the radiator, and then along with x-ray TR photons travel through 2 m helium pipe (the pipe decreases TR scattering and absorption) and the semiconducting pixel or strip detector. The distance between the radiator and detector provides more effective measuring the angular distribution of TR. For simulations we consider 20 GeV electrons and the radiator consisting of 30 foils made of 50 μm Mylar with 2.97 mm air gaps between foils, as well as the 480 μm Si detector — all these correspond to real parameters of a recent experiment [34]. In figure 2 the experimental data [34] are compared with Geant4 simulations for spectral and angular distributions of TR for the Mylar radiator. Here $dN/d(\hbar\omega)$ is the number of photons per photon energy, and $dN/d\theta$ is the number of photons per polar angle of radiation θ.

Figure 2(a) shows that the spectral distribution of TR obtained in Geant4 coincides very well with the experimental one [34]; this should remain in the refined TR module. Unlike the spectral ones, the angular distributions in figure 2(b) coincide only at angles larger than 1 mrad and differ at smaller angles (figure 2(c)). Actually, Geant4 in the present form does not reproduce the fine structure of angular distribution at small angles (see figure 2(c) and comparison with theory in [32]).

3 Correction of Geant4 x-ray TR module

To find the reason why the simulated results differ from experimental and theoretical ones at small angles, we have investigated the main code file responsible for x-ray TR in Geant4

2020 JINST 15 C06024

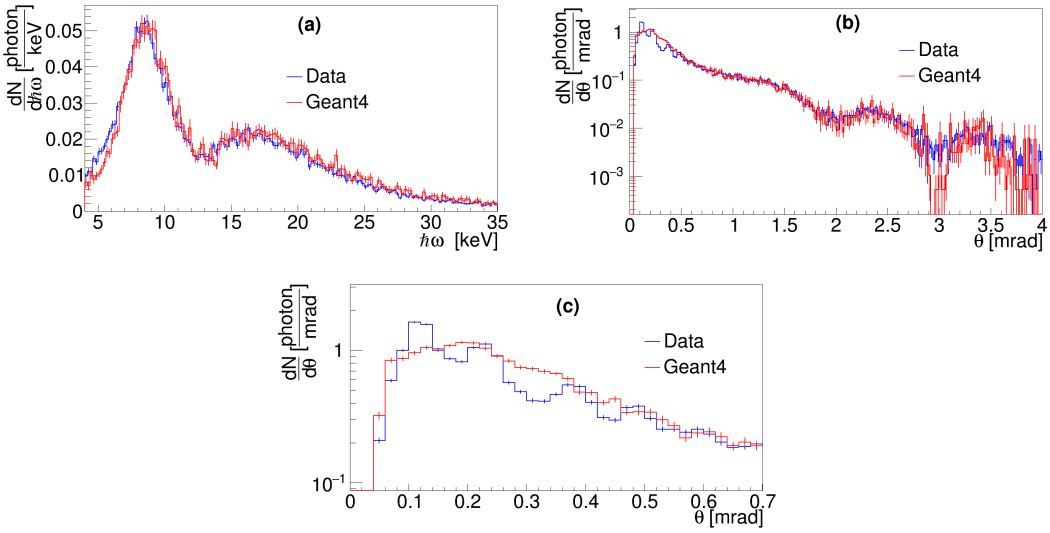

Figure 2. Comparison of the experimental data with Geant4 simulations of (a) spectral and (b, c) angular distribution of x-ray TR photons from 20 GeV electrons after the Mylar radiator, (c) is zoomed part of (b) at small angles. The error bars are shown by vertical lines at the centre of the each histogram bin (the same is about figure 4(a,b)).

`G4VXTRenergyLoss.cc`. In the current 10.6.p01 version of Geant4 angular distributions of TR for regular radiators are calculated in accordance with [31] (with and without TR absorption). In principle, the expressions from the paper [31] should show correct peak positions defined by the dispersion relation for TR [32]:

$$a\omega\left(\gamma^{-2}+\theta^2+\frac{\omega_0^2}{\omega^2}\right)+b\omega\left(\gamma^{-2}+\theta^2+\frac{\omega_{air}^2}{\omega^2}\right)=4\pi cr, \tag{3.1}$$

where γ is the electron Lorentz factor, c is the speed of light, ω_0 and ω_{air} are the plasma frequencies of foil and air, respectively, ω is the radiation frequency, θ is the polar angle of observation, r is an integer, i.e. an angular harmonic number, a and b are foil and gap thicknesses, respectively. Eq. (3.1) can be understood as the result of the interference of the waves emitted by a periodic structure of the radiator, while mathematically it emerges in the process of analytical integration over the frequencies [32] in a way similar to the so-called Jacobian peaks in the particle physics.

Let us turn to the functions responsible for calculation of TR emission angle and its random choosing for further photon tracking. The function `GetAngleXTR` (see code in appendix — A83) returns an approximate value of TR photon angle in some interval smearing the angles near randomly chosen value in the function `GetRandomAngle` (A61). The width of these intervals is determined by the distance between neighboring angular harmonics (A104), which depends on the harmonic number and photon energy. This distance appears to be larger than the width of fine structure of angular distribution at small angles. We have corrected these intervals decreasing them by the factor of 10 (B104), and that was sufficient for the sharp peaks to appear in the Geant4 angular distribution of TR (see figure 3).

After decreasing the interval width, it appeared that there is an "artificial" peak between first harmonic peak and zero angle (see figure 3). We have found out that the reason of this peak is in the

2020 JINST 15 C06024

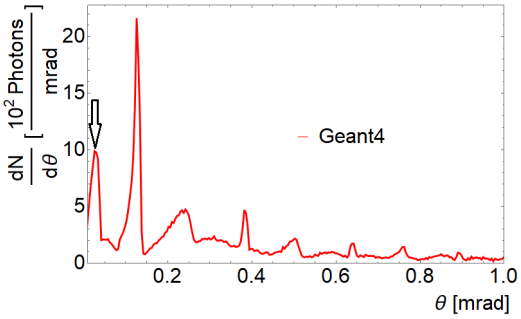

Figure 3. Geant4 angular distribution of x-ray TR photons for 20 GeV electrons crossing the Mylar radiator after decreasing the angular smearing in the code. The "artificial peak" is shown by the arrow.

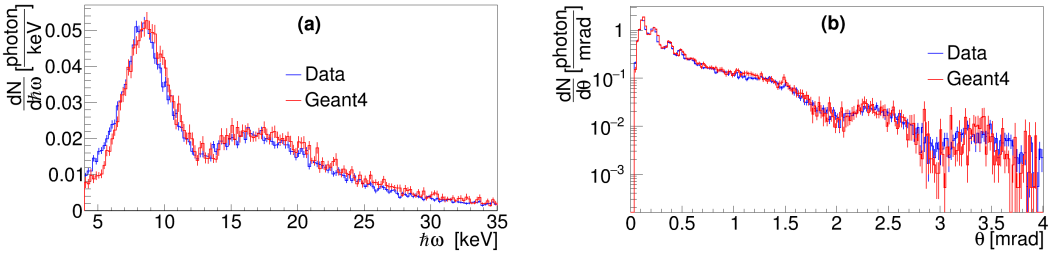

Figure 4. Comparison of experimental data with corrected Geant4 TR module simulations of (a) spectral and (b) angular distribution of x-ray TR photons from and 20 GeV electrons after the Mylar radiator.

`GetAngleVector` (A2) function. In its code, the method for TR angle calculation from [31] was also applied for the TR photons radiated at the small angles between the zero and first harmonics. According to Garibian [17, p. 92], however, for these angles such an approach is not correct and only numerical integration of spectral-angular distribution of TR photons can be applied in this region. On the other side, as the small angles are very close to the primary particle trajectory, we can start the calculations from the first harmonic. Doing so we also eliminate the "artificial" peak. This means that in the original code we should change i) the lines in which the probabilities for the first harmonic and zero angles are determined (A30 and A48): in the original code the first harmonic shares its probability with zero angle — we stop this sharing (B30 and B48); ii) the lines in which loops and conditions use arrays elements for the zero angle (A72, A73, A88): we change all 0 to 1 ("zero harmonics" elements to the first harmonic ones) (B72, B73, B88).

4 Comparison with experiment and theory

After we have applied the corrections to the code of the Geant4 x-ray TR module, the shape of the angular distributions meet our expectations. Figure 4 demonstrates the results of Geant4 simulations for the corrected module compared with the experimental data (the same as in figure 2). The corrected Geant4 x-ray TR module now can reproduce the experimental as well as the theoretical peaks at small angles, see figures 4, 5.

One should notice, however, that there is a small shift of both theoretical spectral and angular distributions relative to Geant4 simulations. We suppose the reason to be in the random sampling

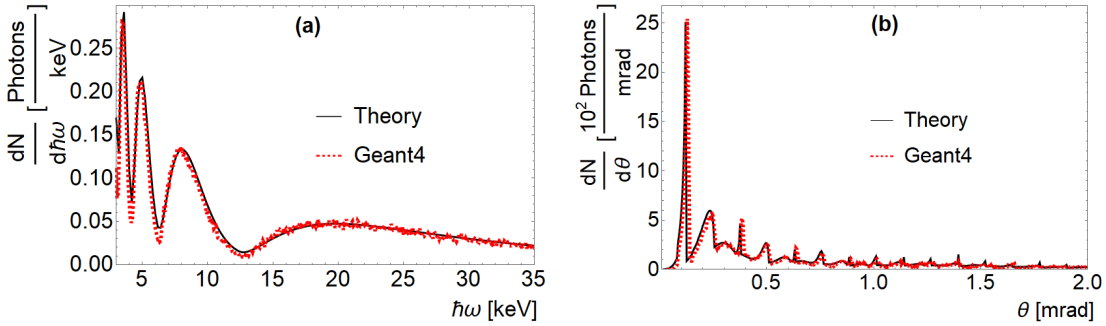

Figure 5. Comparison of refined Geant4 (dashed red line) with theoretical (black solid line) spectral (a) and angular (b) distributions of x-ray TR photons for 20 GeV electrons crossing the Mylar radiator.

procedure of both distributions in Geant4 while theoretical distribution is constructed straight from analytical formulas. Unlike figure 4, figure 5 shows the generated spectrum that does not take into account the absorption in the radiator, for the correct comparison with the theory [32].

5 Conclusion

In this work we have shown how to refine the x-ray TR module in Geant4 so that it gives angular distributions of TR photons coinciding with both theoretical and experimental data. As proposed corrections are rather general, we expect the changes will also be correct for a wide range of parameters, radiators and particles.

The transition radiation simulation developed here can play a vital part for developing detectors capable of detecting ultra-relativistic charged particles with Lorentz factors from 10^3 and above, including hadrons in the TeV energy range, e.g., at the prospective Small Angle Spectrometer [38] (or Forward Hadron Spectrometer [39]) at LHC and other experiments of this kind.

Acknowledgments

This work was supported by the Russian Science Foundation under grant N° 16-12-10277.

A Original code

```
A1   // Vector of angles and angle integral distributions
A2   G4PhysicsFreeVector* G4VXTRenergyLoss::GetAngleVector(G4double energy, G4int n)
A3   {
A4     G4double theta=0., result, tmp=0., cof1, cof2, cofMin, cofPHC, angleSum  = 0.;
A4     G4int iTheta, k, /*kMax,*/ kMin;
A5     G4PhysicsFreeVector* angleVector = new G4PhysicsFreeVector(n);
A6     cofPHC  = 4.*pi*hbarc;
A7     tmp     = (fSigma1 - fSigma2)/cofPHC/energy;
A8     cof1    = fPlateThick*tmp;
A9     cof2    = fGasThick*tmp;
A10    cofMin  =  energy*(fPlateThick + fGasThick)/fGamma/fGamma;
A11    cofMin += (fPlateThick*fSigma1 + fGasThick*fSigma2)/energy;
A12    cofMin /= cofPHC;
```


2020 JINST 15 C06024

```
A13    kMin = G4int(cofMin);
A14    if (cofMin > kMin) kMin++;
A15    if(verboseLevel > 2)
A16    {
A17      G4cout<<"n-1 = "<<n-1<<"; theta = "
A18       <<std::sqrt(fMaxThetaTR)*fGamma<<"; tmp = "
A19       <<0.
A20       <<";    angleSum = "<<angleSum<<G4endl;
A21    }
A22    for( iTheta = n - 1; iTheta >= 1; iTheta-- )
A23    {
A24      k = iTheta - 1 + kMin;
A25      tmp    = pi*fPlateThick*(k + cof2)/(fPlateThick + fGasThick);
A26      result = (k - cof1)*(k - cof1)*(k + cof2)*(k + cof2);
A27      tmp = std::sin(tmp)*std::sin(tmp)*std::abs(k-cofMin)/result;
A28      if( k == kMin && kMin == G4int(cofMin) )
A29      {
A30        angleSum   +=0.5*tmp;
A31      }
A32      else if(iTheta == n-1);
A33      else
A34      {
A35        angleSum   += tmp;
A36       }
A37       theta = std::abs(k-cofMin)*cofPHC/energy/(fPlateThick + fGasThick);
A38       if(verboseLevel > 2)
A39       {
A40         G4cout<<"iTheta = "<<iTheta<<"; k = "<<k<<"; theta = "
A41          <<std::sqrt(theta)*fGamma<<"; tmp = "
A42          <<tmp  <<"; angleSum = "<<angleSum<<G4endl;
A43       }
A44       angleVector->PutValue( iTheta, theta, angleSum );
A45     }
A46     if (theta > 0.)
A47     {
A48       angleSum += 0.5*tmp;
A49       theta = 0.;
A50     }
A51     if(verboseLevel > 2)
A52     {
A53       G4cout<<"iTheta = "<<iTheta<<"; theta = "
A54        <<std::sqrt(theta)*fGamma<<"; tmp = "<<tmp
A55        <<";    angleSum = "<<angleSum<<G4endl;
A56     }
A57     angleVector->PutValue( iTheta, theta, angleSum );
A58     return angleVector;
A59   }
A60   // Get XTR photon angle at given energy and Tkin
A61   G4double G4VXTRenergyLoss::GetRandomAngle( G4double energyXTR, G4int iTkin )
A62   {
A63     G4int iTR, iAngle;
A64     G4double position, angle;
```

```
A65     if (iTkin == fTotBin) iTkin--;
A66     fAngleForEnergyTable = fAngleBank[iTkin];
A67     for( iTR = 0; iTR < fBinTR; iTR++ )
A68     {
A69       if( energyXTR < fXTREnergyVector->GetLowEdgeEnergy(iTR) )  break;
A70     }
A71     if (iTR == fBinTR) iTR--;
A72     position = (*(*fAngleForEnergyTable)(iTR))(0)*G4UniformRand();
A73     for( iAngle = 0;; iAngle++)
A74     {
A75       if( position >= (*(*fAngleForEnergyTable)(iTR))(iAngle) ) break;
A76     }
A77     angle = GetAngleXTR(iTR,position,iAngle);
A78     return angle;
A79   }
A80   // Returns approximate position of x-ray photon angle at given energy during
A81   random sampling
A82   // over integral energy distribution
A83   G4double G4VXTRenergyLoss::GetAngleXTR(G4int iPlace,
A84   G4double position,
A85   G4int iTransfer)
A86   {
A87     G4double x1, x2, y1, y2, result;
A88     if( iTransfer == 0 )
A89     {
A90       result = (*fAngleForEnergyTable)(iPlace)->GetLowEdgeEnergy(iTransfer);
A91     }
A92     else
A93     {
A94       y1 = (*(*fAngleForEnergyTable)(iPlace))(iTransfer-1);
A95       y2 = (*(*fAngleForEnergyTable)(iPlace))(iTransfer);
A96       x1 = (*fAngleForEnergyTable)(iPlace)->GetLowEdgeEnergy(iTransfer-1);
A97       x2 = (*fAngleForEnergyTable)(iPlace)->GetLowEdgeEnergy(iTransfer);
A98       if ( x1 == x2 )    result = x2;
A99       else
A100      {
A101        if ( y1 == y2  ) result = x1 + (x2 - x1)*G4UniformRand();
A102        else
A103        {
A104          result = x1 + (position - y1)*(x2 - x1)/(y2 - y1);
A105        }
A106      }
A107    }
A108    return result;
A109  }
```

B Refined lines

```
...
B28      if( k == kMin && kMin == G4int(cofMin) )
B29      {
B30        angleSum   +=tmp;
B31      }
```


2020 JINST 15 C06024

```
...
B46       if (theta > 0.)
B47       {
B48         angleSum += 0;
B49         theta = 0.;
B50       }
...
B72       position = (*(*fAngleForEnergyTable)(iTR))(1)*G4UniformRand();
B73       for( iAngle = 1;; iAngle++)
...
B88       if( iTransfer == 1 )
...
B104      result = x1 + 0.1*(position - y1)*(x2 - x1)/(y2 - y1);
...
```

References

[1] J. Allison et al., *Recent developments in Geant4*, *Nucl. Instrum. Meth.* **A 835** (2016) 186.

[2] J. Allison et al., *Geant4 developments and applications*, *IEEE Trans. Nucl. Sci.* **53** (2006) 270.

[3] GEANT4 collaboration, *GEANT4 — a Simulation toolkit*, *Nucl. Instrum. Meth.* **A 506** (2003) 250.

[4] D.D. DiJulio et al., *High-energy in-beam neutron measurements of metal-based shielding for accelerator-driven spallation neutron sources*, *Phys. Rev. ST-AB* **19** (2016) 053501.

[5] G. Alexander et al., *Observation of polarized positrons from an undulator-based source*, *Phys. Rev. Lett.* **100** (2008) 210801.

[6] U. Husemann, J. Mechnich and A. Salzburger, *Simulation strategies using FATRAS and GEANT4 for a future upgrade of the ATLAS tracking*, *J. Phys. Conf. Ser.* **219** (2010) 032021.

[7] D. Costanzo et al., *The GEANT4-based simulation software of the ATLAS detector*, *IEEE Nucl. Sci. Symp. Conf. Rec.* **5** (2006).

[8] ATLAS collaboration, *The ATLAS simulation infrastructure*, *Eur. Phys. J.* **C 70** (2010) 823 [arXiv:1005.4568].

[9] K. Abdel-Waged, N. Felemban and V.V. Uzhinskii, *GEANT4 hadronic cascade models analysis of proton and charged pion transverse momentum spectra from p + Cu and Pb collisions at 3, 8 and 15 GeV/c*, arXiv:1012.4165.

[10] Y. Takubo, R.N. Hodgkinson, K. Ikematsu, K. Fujii, N. Okada and H. Yamamoto, *Measuring anomalous couplings in $H \to WW^*$ decays at the International Linear Collider*, *Phys. Rev.* **D 88** (2013) 013010 [arXiv:1011.5805].

[11] I. Agapov et al., *Tracking studies of the Compact Linear Collider collimation system*, *Phys. Rev. ST-AB* **12** (2009) 081001.

[12] F. Berg et al., *Target studies for surface muon production*, *Phys. Rev. ST-AB* **19** (2016) 024701 [arXiv:1511.01288].

[13] S. Incerti et al., *Review of GEANT4-DNA applications for micro and nanoscale simulations*, *Phys. Med.* **32** (2016) 1187.

[14] M.B. Hahn et al., *Measurements and simulations of microscopic damage to DNA in water by 30 keV electrons: a general approach applicable to other radiation sources and biological targets*, *Phys. Rev.* **E 95** (2017) 052419.

2020 JINST 15 C06024

[15] K. Murase, K. Ioka, S. Nagataki and T. Nakamura, *High-energy cosmic-ray nuclei from high- and low-luminosity gamma-ray bursts and implications for multi-messenger astronomy*, *Phys. Rev.* **D 78** (2008) 023005 [arXiv:0801.2861].

[16] KamLAND collaboration, *Production of radioactive isotopes through cosmic muon spallation in KamLAND*, *Phys. Rev.* **C 81** (2010) 025807 [arXiv:0907.0066].

[17] G.M. Garibian and C. Yang, *X-ray transition radiation* (in Russian), Yerevan, Armenia (1983).

[18] V.L. Ginzburg and I.M. Frank, *Radiation of a uniformly moving electron due to its transition from one medium into another*, *J. Phys. (USSR)* **9** (1945) 353.

[19] M.L. Cherry, G. Hartmann, D. Muller and T.A. Prince, *Transition radiation from relativistic electrons in periodic radiators*, *Phys. Rev.* **D 10** (1974) 3594.

[20] M.L. Cherry, *Measurements of the spectrum and energy dependence of x-ray transition radiation*, *Phys. Rev.* **D 17** (1978) 2245.

[21] B. Dolgoshein, *Transition radiation detectors*, *Nucl. Instrum. Meth.* **A 326** (1993) 434.

[22] P. Nevski, *Advances in the simulation of transition radiation detectors*, *Nucl. Instrum. Meth.* **A 522** (2004) 116.

[23] X. Artru, G.B. Yodh and G. Mennessier, *Practical theory of the multilayered transition radiation detector*, *Phys. Rev.* **D 12** (1975) 1289.

[24] AMS-TRD collaboration, *The AMS TRD. A gasdetector designed for operation in space*, *Nucl. Phys. Proc. Suppl.* **B 150** (2006) 30.

[25] ATLAS TRT collaboration, *The ATLAS TRT end-cap detectors*, 2008 *JINST* **3** P10003; *The ATLAS TRT barrel detector*, 2008 *JINST* **3** P02014.

[26] ATLAS collaboration, *The ATLAS experiment at the CERN Large Hadron Collider*, 2008 *JINST* **3** S08003.

[27] ALICE collaboration, *The ALICE experiment at the CERN LHC*, 2008 *JINST* **3** S08002.

[28] J. Apostolakis et al., *Parameterization models for X-ray transition radiation in the GEANT4 package*, *Comput. Phys. Commun.* **132** (2000) 241.

[29] V.M. Grichine, *Generation of X-ray transition radiation inside complex radiators*, *Phys. Lett.* **B 525** (2002) 225.

[30] V.M. Grishine and S.S. Sadilov, *GEANT4 models for X-ray transition radiation*, *Nucl. Instrum. Meth.* **A 522** (2004) 122.

[31] V.M. Grichine, *Angular distribution of X-ray transition radiation from regular radiators*, *Nucl. Instrum. Meth.* **A 696** (2012) 141.

[32] A.A. Savchenko, D. Yu. Sergeeva, A.A. Tishchenko and M.N. Strikhanov, *Small-angle x-ray transition radiation from multilayered structures*, *Phys. Rev.* **D 99** (2019) 016015.

[33] P. Goedtkindt et al., *Interference effects in x-ray transition radiation with a 500 MeV electron beam*, *Nucl. Instrum. Meth.* **B 56** (1991) 1060.

[34] E.J. Schioppa et al., *First measurements of the spectral and angular distribution of transition radiation using a silicon pixel sensor on a Timepix3 chip*, *Nucl. Instrum. Meth.* **A 936** (2019) 523.

[35] J. Alozy et al., *Studies of the spectral and angular distributions of transition radiation using a silicon pixel sensor on a Timepix3 chip*, *Nucl. Instrum. Meth.* **A 961** (2020) 163681.

2020 JINST 15 C06024

[36] J. Alozy et al., *Identification of particles with Lorentz factor up to* 10^4 *with Transition Radiation Detectors based on micro-strip silicon detectors*, *Nucl. Instrum. Meth.* **A 927** (2019) 1 [arXiv:1901.11265].

[37] F. Dachs et al., *Transition radiation measurements with a Si and a GaAs pixel sensor on a Timepix3 chip*, *Nucl. Instrum. Meth.* **A 958** (2020) 162037.

[38] *First meeting on Small Angle Spectrometer at LHC*, at https://indico.cern.ch/event/435373/.

[39] M. Albrow, *A very forward hadron spectrometer for the LHC and cosmic ray physics*, PoS(EDSU2018)048 [arXiv:1811.02047].

2020 JINST 15 C06024